NANO LETTERS

2007
Vol. 7, No. 6
1711−1716

Simultaneous Multicolor Imaging of Five Different Lymphatic Basins Using Quantum Dots

Hisataka Kobayashi,*,† Yukihiro Hama,† Yoshinori Koyama,† Tristan Barrett,† Celeste A. S. Regino,‡ Yasuteru Urano,§ and Peter L. Choyke†

Molecular Imaging Program and Radiation Oncology Branch, Center for Cancer Research, National Cancer Institute, Bethesda, Maryland 20892-1088, and Graduate School of Pharmaceutical Sciences, The University of Tokyo, 7-3-1 Hongo, Bunkyo-ku, Tokyo 113-0033, Japan

Received March 26, 2007; Revised Manuscript Received May 8, 2007

ABSTRACT

Quantum dots can be used to perform multicolor images with high fluorescent intensity and are of a nanosize suitable for lymphatic imaging via direct interstitial injection. Here simultaneous multicolor in vivo wavelength-resolved spectral fluorescence lymphangiography is shown using five quantum dots with similar physical sizes but different emission spectra. This allows noninvasive and simultaneous visualization of five separate lymphatic flows draining and may have implications for predicting the route of cancer metastasis into the lymph nodes.

The lymphatic system is difficult to evaluate because its channels are small and not directly accessible. Moreover, when assessing lymphatic drainage from more than two separate drainage basins, techniques such as X-ray lymphangiography, MR lymphangiography, or radionuclide radioscintigraphy should repeatedly study each separately, one at a time, with appropriate intervals because it is impossible to differentiate the contributions from each lymphatic basin. Quantum dots (Qdots) are characterized by sharply defined emission spectra and can be synthesized to emit a variety of wavelengths.[1] Qdots can vary in size, but all are of nanosize and some of them have appropriate sizes to conduct lymphatic tracking studies using intracutaneous injection, as demonstrated by prior studies using macromolecular dendrimer particles on MRI.[2,3] Kim et al. reported successful in vivo imaging of the lymphatics using a near-infrared (NIR) Qdot in order to detect the sentinel lymph node (SLN) arising from breast tissue.[4] Multicolor imaging is a known application of in vitro microscopic imaging. These in vitro microscope studies are performed using either exogenous florescent probe combinations of fluorescein, rhodamine, cyanine dyes, or endogenous fluorescent protein combinations of green, yellow, and red fluorescent proteins.[5] The images are taken separately, one color at a time with an appropriate filter set, and then the colors are merged at postprocessing to compose a multicolor image. Simultaneous, more than three-color imaging using a single excitation source is only possible using either Qdots[1] or the Keima series of fluorescent proteins[6] as fluorescence sources, combined with the spectral-resolved technique. The depth of the target makes in vivo fluorescence imaging generally more difficult than in vitro imaging. Therefore, to date, only few in vivo two-color imaging studies have been reported for visualizing two separate physiological functions using exogenous florescent probes.[7,8]

Imaging using five colors in vivo has rarely been performed. We employed five carboxyl cadmium−selenium (Cd−Se; 565, 605, and 655 peak emission) or cadmium−tellurium (Cd−Te; 705 and 800 peak emission) Qdots of similar sizes with different emission spectra. In brief, carboxyl quantum dots, Qdot 565 ITK, Qdot 605 ITK, Qdot 655 ITK, Qdot 705 ITK, and Qdot 800 ITK (peak emission wavelength at 565, 605, 655, 705, and 800 nm, respectively) were selected among Qdots with various surface coatings because of their appropriate hydrodynamic sizes for the lymphatic imaging, as shown below and purchased from Invitrogen Corporation (Carlsbad, CA).

Size analysis of all five Qdots was performed with the dynamic light scattering (DLS) and gel filtration for hydrodynamic size, and a transmission electron microscope (TEM) for metal cores as summarized in Table 1. Briefly, DLS was performed using a Malvern Zeta Sizer Nano instrument

* Corresponding author. E-mail: Kobayash@mail.nih.gov. Molecular Imaging Program, Center for Cancer Research, NCI/NIH, Building 10, Room 1B40, MSC 1088, Bethesda, Maryland 20892-1088.

† Molecular Imaging Program, Center for Cancer Research, National Cancer Institute.

‡ Radiation Oncology Branch, Center for Cancer Research, National Cancer Institute.

§ Graduate School of Pharmaceutical Sciences, The University of Tokyo.

10.1021/nl0707003 CCC: $37.00
Published on Web 05/26/2007

Table 1. Physical and Hydrodynamic Size Analysis of Five Carboxyl QDS

QDs/methods	QD 565 (Cd/Se)	QD 605 (Cd/Se)	QD 655 (Cd/Se)	QD 705 (Cd/Te)	QD 800 (Cd/Te)
DLS[a] (diameter in nm)	15.0 ± 6.0	15.4 ± 4.3	ND[1]	ND[1]	16.9 ± 7.3
TEM[b] (diameter in nm)	7.8 ± 0.5	10.3 ± 0.5	13.4 ± 0.7	9.7 ± 0.3	12.0 ± 0.5
HPLC[c] elution time (min)	17.24 ± 0.01	17.01 ± 0.01	16.85 ± 0.01	16.97 ± 0.01	16.85 ± 0.00
diameter (nm)	(16.3 nm)	(17.1 nm)	(18.9 nm)	(18.0 nm)	(18.8 nm)

[a] Not determined: data is not reliable because of the fluorescence contamination in the signal. [b] TEM: sizes of well-separated 50 particles in each sample were measured. [c] Standard proteins: IgM (24.2 nm); 16.08 ± 0.00, thyroglobulin; (17.0 nm); 17.11 ± 0.01 min, IgG (11.0 nm); 18.17 ± 0.00 min.

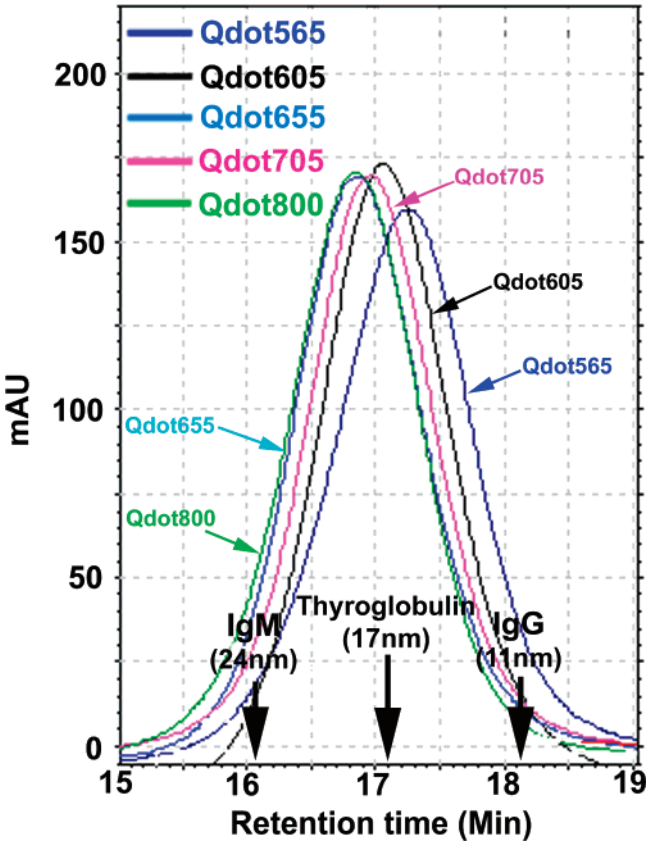

Figure 1. Hydrodynamic sizes of five carboxyl Qdots range from 15 to 19 nm in diameter. Size-exclusion HPLC traces of five Qdots using TSK G6000PW column. IgM (24 nm), thyroglobulin (17 nm), and IgG (11 nm) were used as reference molecules.

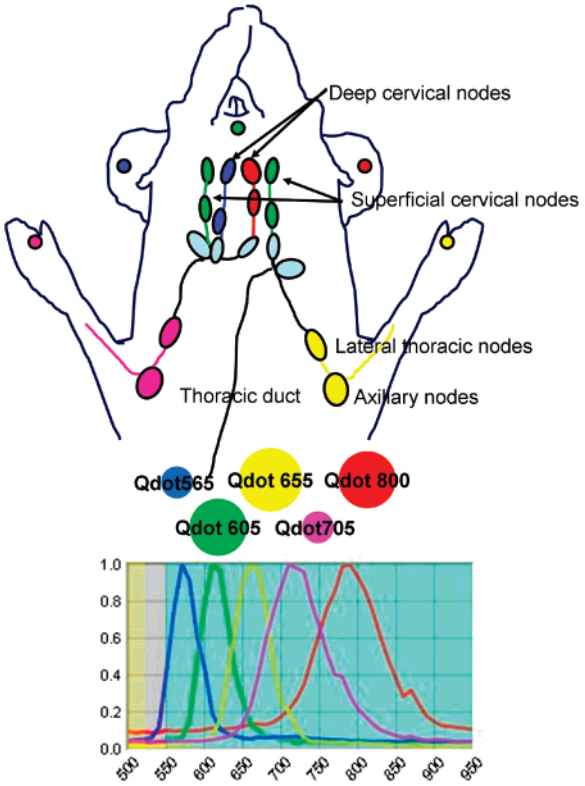

Figure 2. Anatomy of the lymphatic system in the upper body of the mouse and a schematic illustration of five-color spectral fluorescence imaging, with a graph of the emission spectra of each of the five carboxyl quantum dots used (Qdot 565, blue; Qdot 605, green; Qdot 655, yellow; Qdot 705, magenta; Qdot 800, red). The colored lymph nodes are the draining lymph nodes visualized in this study.

(Malvern Instruments Ltd., Malvern, UK) in NanoComposix, Inc., (San Diego, CA). We repeated the examination five times in order to accurately obtain the size measurements. Gel filtration was performed using a high-performance liquid chromatography (System Gold, Beckman Coulter, Inc., Fullerton, CA), equipped with TSK G6000PW 30 cm column (Tosoh Bioscience LLC, Montgomeryville, PA), consisting of 17 μm hydroxylated polymethacrylate particles with >100 nm pores. All Qdots and standard samples (IgM 25 nm, thyroglobulin 17 nm and IgG 11 nm) were eluted with 0.066M PBS (Figure 1). The gel filtration results were validated using two other columns: Shodex KW405-4F 30 cm (Showa Denko America, Inc., New York, NY) and TSK G2000SW 60 cm (Tosoh Bioscience LLC), and similar results were obtained. The TEM images were taken with a JEOL 200 kV instrument (JEOL USA, Inc., Peabody, MA) with a 4 megapixel CCD camera in NanoComposix, Inc., and obtained images were calibrated as 1.44 pixels/nm. Fifty well-separated and focused particles were randomly selected in the magnified view, and the pixel numbers of their long diameters were counted to calculate their size.

We simultaneously injected five or four Qdots intracutaneously into five different sites in the middle phalanges, the upper extremity, the ears, and the chin, in order to monitor the lymphatic drainages in the neck and the upper trunk, where the most complicated lymphatic networks exist in the body (Figure 2). In brief, all in vivo procedures were carried out in compliance with the Guide for the Care and Use of Laboratory Animal Resources (1996), National Research Council, and approved by the National Cancer Institute Animal Care and Use Committee. Ten-week-old normal athymic female mice were anaesthetized via intraperitoneal injection of 1.15 mg sodium pentobarbital (Dainabot, Osaka, Japan). Five consecutive mice were administered intracutaneous injections of 10 μL (24 pmol for Qdot 565 or 12 pmol

Table 2. Summary of Injection Pattern for In Vivo Five-Color and Four-Color Spectral Fluorescence Lymphatic Imaging

animal no.	right hand	left hand	right ear	left ear	median chin
1	705	605	565	655	800
2	565	800	605	705	655
3	605	705	800	655	565
4	655	565	705	800	605
5	800	655	605	565	705
6	655	705	605	800	
7	800	655	705	605	
8	605	800	655	705	
9	705	800	605	655	
10	605	655	800	705	

for other four Qdots) of each Qdot solution (Qdot 565, Qdot 605, Qdot 655, Qdot 705, and Qdot 800) into one of five sites: the middle phalange of the left or right upper extremity, the left or right ear, and the median chin. Another five consecutive mice were given intracutaneous 10 μL (12 pmol) injections of each Qdot solution (Qdot 605, Qdot 655, Qdot 705, and Qdot 800), prepared as above, into either one of four sites: the middle phalange of the left or right upper extremity, and the left or right ear. Injection points were rotated in each mouse, as shown in Table 2. Within 5 min after injection of the Qdots, wavelength-resolved spectral imaging was carried out using a spectral imaging system (Maestro In-Vivo Imaging System, CRI Inc., Woburn, MA). Animals were placed in the spinal position while under pentobarbital anesthesia. The injection sites were masked with a nonfluorescent black tape because the signal from the injection site would otherwise overwhelm the dynamic range of the camera, rendering the unmixing algorithm nonfunctional. After obtaining in vivo images, lymphadenectomy was performed and another spectral fluorescence image was obtained during surgery. All removed LNs were validated using ex vivo spectral fluorescence imaging. Excitation band-pass filters of 445−490 nm for the five-color study and 480−520 nm for the four-color study were used. The tunable filter was automatically stepped in 10 nm increments from 500 to 950 nm using the same exposure time for images captured at each wavelength. Collected images were analyzed by the Maestro software, which uses spectral unmixing algorithms to separate autofluorescence from quantum dot signals, and a composite image consisting of all five Qdot signals and autofluorescence was generated using a spectral library obtained from each one of injected Qdot solutions.

Five-color fluorescence lymphangiography following injections of one of Qdot 565, 605, 655, 705, and 800 in the upper extremities and ears also successfully visualized the lymphatic drainages to the primary lymph nodes in all five mice using spectral fluorescence imaging (Figures 3a, 4a). However, we needed to use a double dose of Qdot 565 because of its weak emission within the high autofluorescence background at 565 nm. All draining lymph nodes were validated by ex vivo fluorescence images of resected LNs (Figures 3b, 4b, Supporting Information movie). Using the Qdots 605, 655, 705, and 800 in the upper extremities and ears, and rotating the sequence of injection in successive mice, allowed visualization of all draining lymph nodes in all mice (mice nos. 6−10 in Table 2) at the same time.

Prior results with gadolinium-labeled dendrimer-based nanoparticles suggest that relatively large nanoparticles, ≥13 nm diameter, were optimal for visualizing the regional lymphatics following intracutaneous injection.[9] The hydrodynamic diameter of all carboxyl Qdots was approximately 15−19 nm in diameter, which is larger than albumin (~6 nm) but much smaller than Sn-colloid, macroaggregated albumin, or microbubble contrast agents for ultrasonography, which have diameters ranging from 100 to 5000 nm and are currently used for the sentinel node imaging. Large molecules do not efficiently move from the injection site and necessitate massage at the injection site.[10] Therefore, for depicting lymphatic drainage imaging by intracutaneous injection, these carboxyl Qdots approximate the optimal hydrodynamic size range for the drainage pharmacokinetics. In terms of washout from the primary draining LNs, Qdots stayed at the first draining LN longer than NIR-dye-labeled immunoglobulin G (IgG) or dendrimers with similar hydrodynamic sizes. NIR-labeled IgG and Gd-labeled dendrimer showed peak accumulation within 1 h postinjection.[3,11] In contrast, these carboxyl Qdots did not show a noticeable decrease in fluorescence signal for up to 3 h postinjection and rarely showed up in the secondary draining LNs. Therefore, carboxyl Qdots may provide a longer time frame after injection in which to identify the sentinel node, as compared to other reagents. Despite successful five-color imaging, the Qdot 565 should be injected at a double dose. The lower brightness and less penetration of emitted light of Qdot 565 with its green fluorescence compared with the other four Qdots compelled us to use a large injection dose. In addition, four-color fluorescence lymphangiography using the Qdots 605, 655, 705, and 800 in the upper extremities and ears and rotating the sequence of injection in successive mice allowed visualization of all draining lymph nodes in all mice (mice nos. 6−10 in Table 2). These results suggest that Qdots with emission around 750 nm may be a better alternative to Qdot 565 as a fifth Qdot for five-color imaging if the size is appropriate.

The practical implication of this study is that it is possible to separately study the drainage patterns and mixing of five adjacent lymphatic basins in vivo using high-resolution imaging in the laboratory environment. This method has the potential to analyze five independent parameters in a single shot during an in vivo small animal image. Qdot imaging could potentially assist in the understanding of lymphatic drainage patterns, especially for complicated regions such as in the head and neck. In this study, all major drainage trunks (bilateral, superficial, deep cervical trunks, and trunks from bilateral upper extremities) of the lymphatics in the upper body in the mouse can be depicted separately on five-color images. The lymphatic system in the head and neck region of humans is even more complicated than in the mouse, thus more than five colors may need to be employed. Although this method does not yet have practical clinical application, it is possible that this technology will enable

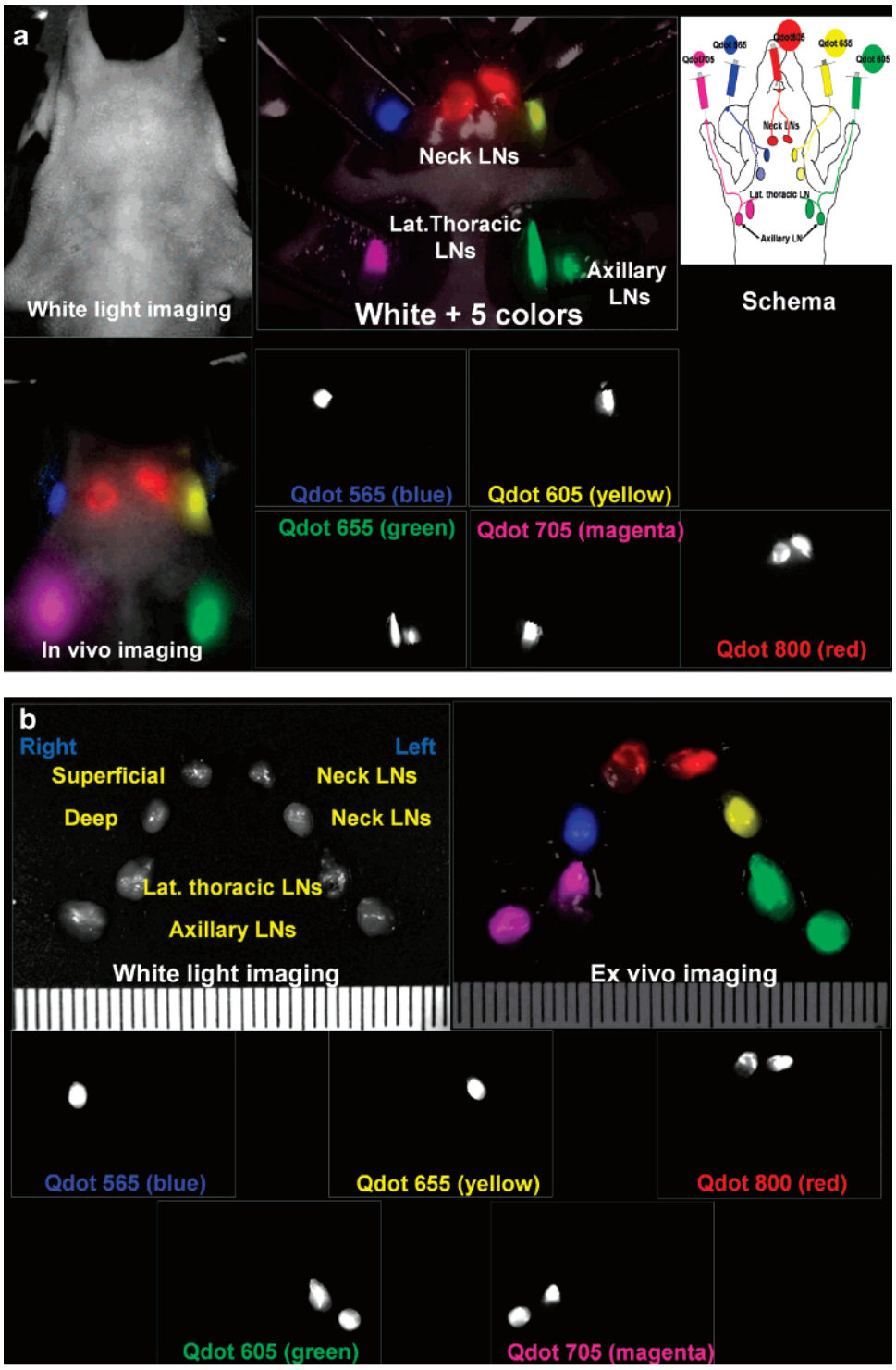

Figure 3. In vivo five-color lymphatic drainage imaging was able to visualize five distinct lymphatic drainages. (a) In vivo and intrasurgical spectral fluorescence imaging of a mouse injected with five carboxyl Qdots (565, blue; 605, green; 655, yellow; 705, magenta; 800, red) intracutaneously into the middle digits of the bilateral upper extremities, the bilateral ears, and at the median chin, as shown in the schema (mouse no. 1 in Table 2). Five primary draining lymph nodes were simultaneously visualized with different colors through the skin in the in vivo image and are more clearly seen in the image taken at the surgery. (b) Ex vivo spectral fluorescence imaging of the eight draining lymph nodes after surgical resection.

procedures that relay on independently identifying different lymphatic basins. Another potential adaptation of this method is the simultaneous, but separate, in vivo monitoring of cellular trafficking. Various immune cells (including T-cell subtypes and dendritic cells) can be labeled by different Qdots with distinct colors to allow in vivo tracking of the cells, which may be of interest for future immunological research in physiological and/or pathophysiological states. The carboxyl Qdots used in our experiments contain cadmium; toxicity of Qdots is an active area of research.[12,13] The toxicity profile of Qdots and the safe dose for administration (in picomoles) needs to be quantified before human

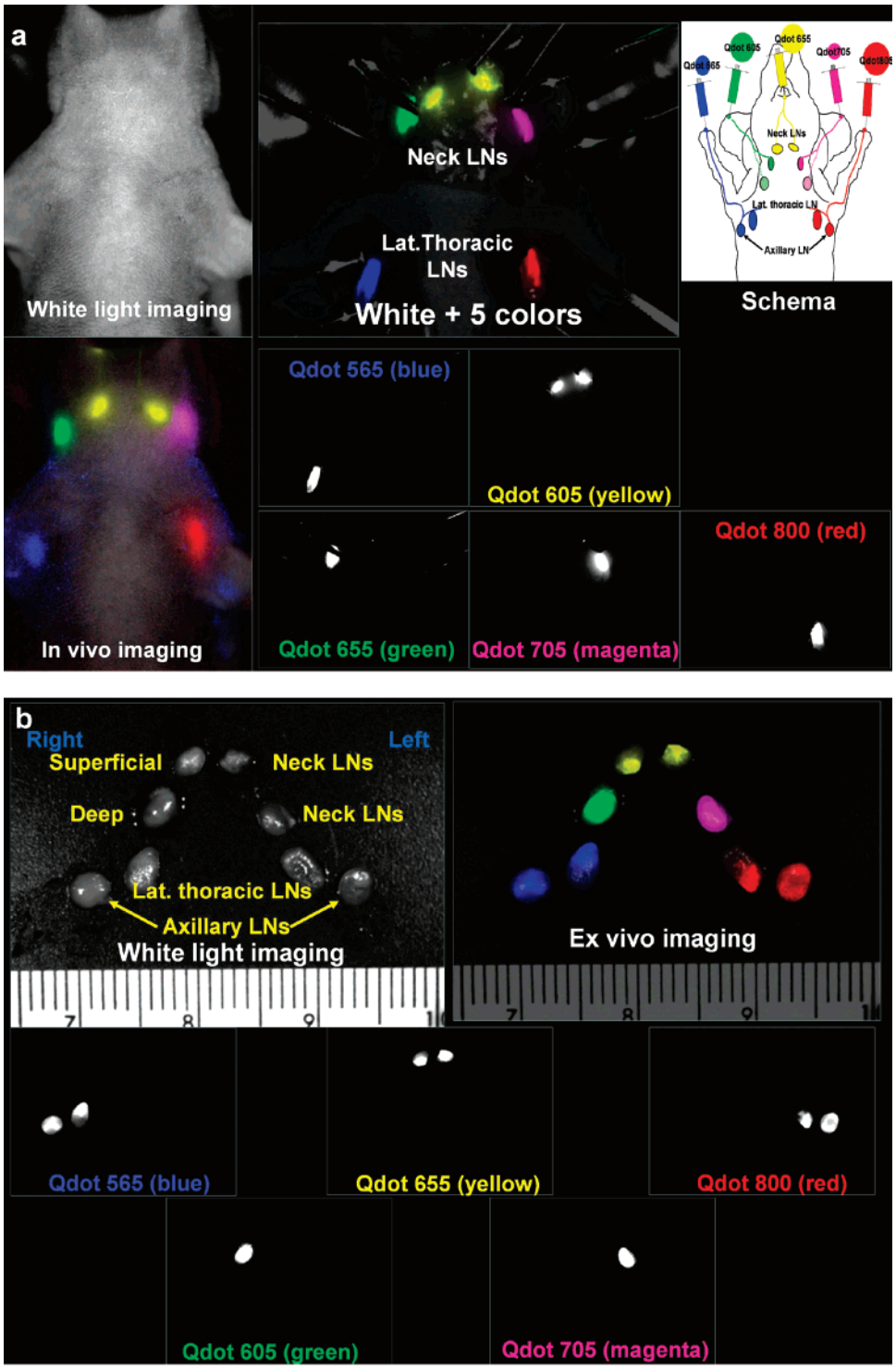

Figure 4. Consistent visualization of lymphatic drainage, even after shuffling the pattern of injection sites. (**a**) In vivo and intrasurgical spectral fluorescence imaging of a mouse injected with five carboxyl Qdots (565, blue; 605, green; 655, yellow; 705, magenta; 800, red) intracutaneously into the middle digits of the bilateral upper extremities, the bilateral ears, and at the median chin, at different locations from mouse no. 1 in Figure 2, as shown in the schema (mouse no. 2 in Table 2). Five primary draining lymph nodes were simultaneously visualized with different colors through the skin in the in vivo image, and more clearly seen in the image taken at the surgery. (b) Ex vivo spectral fluorescence imaging of the eight draining lymph nodes after surgical resection.

studies can be undertaken. If such studies find Qdots unsuitable for human use, alternative dyes will need to be developed and tested. However, it should be noted that the wider bandwidth of organic dyes makes them less suitable in this instance, and it is unlikely that five distinct lymphatic basins can be simultaneously visualized, nevertheless, 2−3 separate dyes could potentially be resolved. However, this method could still be an excellent research tool for the study of lymphatic biology and immunology.

To our knowledge, this is the first demonstration of the simultaneous imaging of five different lymphatic flows in vivo and their trafficking to distinct lymph nodes. Further-

more, carboxyl Qdots hold excellent potential as an imaging method for the exploration of the lymphatic system because of their appropriate size range.

Acknowledgment. This research was supported by the Intramural Research Program of the NIH, National Cancer Institute, Center for Cancer Research.

Supporting Information Available: A movie (AVI) demonstrating multicolor spectral fluorescence imaging during surgery in mouse no. 2, as shown in Figure 3a. A series of spectral fluorescence images, which were captured in 10 nm increments from 500 to 950 nm with a 3 ms exposure at each wavelength, are shown as a movie. Each lymph node is glowing at a different wavelength that is consistent with color and unmixed images, as shown in Figure 3a. This material is available free of charge via the Internet a http://pubs.acs.org.

References

(1) Goldman, E. R.; Clapp, A. R.; Anderson, G. P.; Uyeda, H. T.; Mauro, J. M.; Medintz, I. L.; Mattoussi, H. *Anal. Chem.* **2004**, *76*, 684.
(2) Kobayashi, H.; Kawamoto, S.; Choyke, P. L.; Sato, N.; Knopp, M. V.; Star, R. A.; Waldmann, T. A.; Tagaya, Y.; Brechbiel, M. W. *Magn. Reson. Med.* **2003**, *50*, 758.
(3) Kobayashi, H.; Kawamoto, S.; Bernardo, M.; Brechbiel, M. W.; Knopp, M. V.; Choyke, P. L. *J. Controlled Release* **2006**, *111*, 343.
(4) Kim, S.; Lim, Y. T.; Soltesz, E. G.; De Grand, A. M.; Lee, J.; Nakayama, A.; Parker, J. A.; Mihaljevic, T.; Laurence, R. G.; Dor, D. M.; Cohn, L. H.; Bawendi, M. G.; Frangioni, J. V. *Nat. Biotechnol.* **2004**, *22*, 93.
(5) Hoffman, R. M. *Nat. Rev. Cancer* **2005**, *5*, 796.
(6) Kogure, T.; Karasawa, S.; Araki, T.; Saito, K.; Kinjo, M.; Miyawaki, A. *Nat. Biotechnol.* **2006**, *24*, 577.
(7) Hama, Y.; Koyama, Y.; Urano, Y.; Choyke, P. L.; Kobayashi, H. *Breast Cancer Res. Treat.* **2007**, *103*, 23.
(8) Gao, X.; Cui, Y.; Levenson, R. M.; Chung, L. W.; Nie, S. *Nat. Biotechnol.* **2004**, *22*, 969.
(9) Kobayashi, H.; Kawamoto, S.; Sakai, Y.; Choyke, P. L.; Star, R. A.; Brechbiel, M. W.; Sato, N.; Tagaya, Y.; Morris, J. C.; Waldmann, T. A. *J. Natl. Cancer Inst.* **2004**, *96*, 703.
(10) Choi, S. H.; Kono, Y.; Corbeil, J.; Lucidarme, O.; Mattrey, R. F. *Am. J. Roentgenol.* **2004**, *183*, 513.
(11) Hama, Y.; Koyama, Y.; Urano, Y.; Choyke, P. L.; Kobayashi, H. *J. Invest. Dermatol.* **2007**, in press.
(12) Hardman, R. *Environ. Health Perspect.* **2006**, *114*, 165.
(13) Zhang, T.; Stilwell, J. L.; Gerion, D.; Ding, L.; Elboudwarej, O.; Cooke, P. A.; Gray, J. W.; Alivisatos, A. P.; Chen, F. F. *Nano Lett.* **2006**, *6*, 800.

NL0707003